Data Processing for Broadband Relay Satellite Networks – Digital Architecture and Performance Evaluation

Bernd Friedrichs

Tesat Spacecom GmbH & Co. KG, Gerberstrasse 49, 71522 Backnang, Germany
bernd.friedrichs@tesat.de

In a relay satellite network, information from LEO satellites is transmitted first over an OISL (Optical InterSatellite Link) to a GEO relay satellite and then via microwave Ka-band from the GEO relay to the GS (Ground Station). ESA and ASV (Astrium Services) have initiated the program EDRS (European Data Relay Satellite) for the development and operation of several GEO relay satellites. This paper covers the digital concepts for packet data transmission with up to 1800 Mbps in the complete network LEO→GEO→GS. The LEO contains a digital processing unit where the outputs of several mass memories are encapsulated into packets, error-control coding is added and finally multiplexing and frame stuffing is applied to generate a data stream for the transmission over the OISL. Another digital processing unit is located in the GEO relay, where the data stream received from the OISL is again encapsulated and packetized, encrypted, encoded, multiplexed with idle frames and split to several Ka-band DL (DownLink) channels. The performance of the network is evaluated by a combination of analytical and simulation methods.

I. Introduction

This paper covers digital design aspects and performance evaluation methods for broadband data transmission systems over GEO data relay satellites (Geostationary Earth Orbit). Data from earth observation LEO satellites (Low Earth Orbit) is transmitted in a first step via an OISL (Optical InterSatellite Link) to the GEO relay where both spacecrafts are equipped with LCTs (Laser Communication Terminal). In a second step, the data is transmitted from GEO to GS (Ground Station) via one or several microwave feeder DLs (DownLink), typically operating in the Ka-band. The whole setup can be considered as a satellite network in general and the GEO relay is operated as a regenerative repeater in particular, dominated by digital OBP (On-Board Processing) between laser link and microwave RF downlink.

In order to achieve maximum independence between LEO and GEO satellites, and between the MM (Mass Memory) of the LEO and the LCT, all data is packetized in multiple stages where source frames are encapsulated by (super)frames in the LEO and (super)frames are encapsulated by (hyper)frames in the GEO.

In contrast to the well-known properties of the RF link, the transmitting and receiving LCTs of the OISL are exposed to microvibrations, where vibrations as well as the optical beam angle are in the order of few µrads (micro-radiant). The vibration spectra of LEO and GEO satellites are available (based on mechanical analysis) and then converted into a time-variant discrete-time model of the optical link, taking into account the pointing-tracking control-loop properties of the LCTs and all other relevant effects of optical receivers [6,7].

With models for error patterns for the time-variant optical and microwave links, further challenges have to be mastered to enable the simulation of very low FER (Frame Error Rate) in reasonable times. Decoding failures are one source of errors after receiver processing, however, some specific effects are caused in the receiver by reverting staggered packet encapsulation and frame stuffing. The latter requires increased signal processing for de-stuffing on ground to avoid catastrophic error propagation in case of packet

misclassification. The simulation is supplemented with analytical calculations for the prediction of asymptotically low error rates. Results available so far help to identify those components in the satellite network with major impact.

II. GEO Relay Satellites and Hybrid Payloads

Depending on orbit heights and inclination, the contact time between LEO and a fixed GS (Ground Station) is limited to a few minutes in best case. The problem can be relaxed with several GS, but this is an extensive approach also requiring a dedicated extensive ground network.

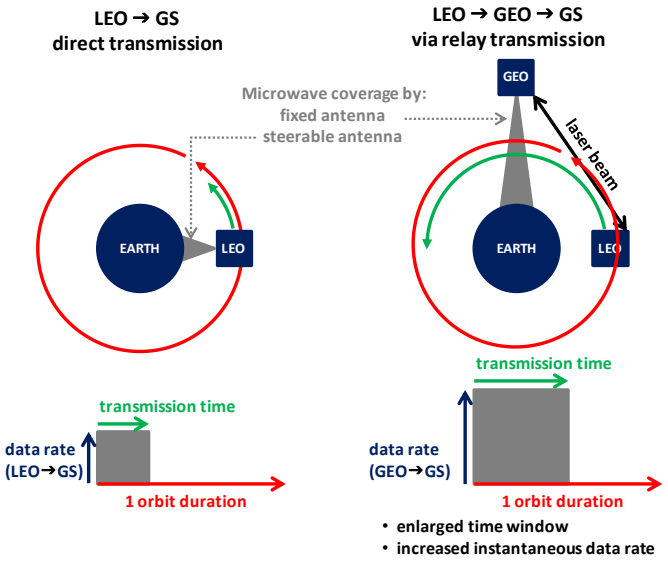

Fig. 1: Options for LEO connection ("directly to GS" versus "via GEO relay")

The contact time to a LEO can be extended to half of the orbit duration if a GEO relay satellite is available as demonstrated in Fig. 1. Data is transmitted firstly over an ISL from the LEO satellite to the GEO relay and then secondly over a DL from GEO to GS. The DL is also referred to as feeder DL and can be operated with a high data rate and high availability. The GEO relay does not need any steerable antenna in contrast to LEO satellites transmitting directly to GS.

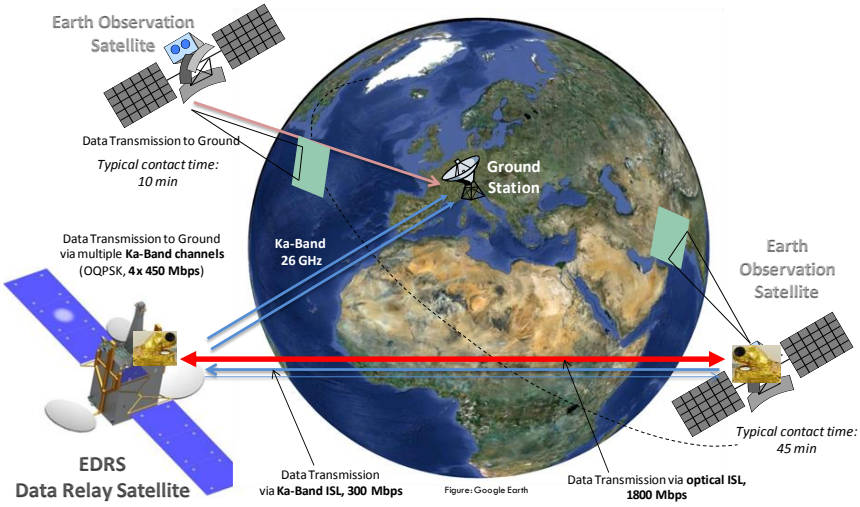

Fig. 2: Operation of the EDRS relay satellite

The EDRS mode of operation is shown in Fig. 2. Two GEO spacecrafts EDRS-A and EDRS-C [12] will be placed at different orbit positions. They are built up with different platforms but identical data processing. A family of LEO satellites (known as Sentinel satellites [8]) are also under development in the context of the GMES (Global Monitoring for Environment and Safety) initiative of ESA (European Space Agency) [4,5].

LEO satellites as used for earth observation purposes are producing typically high amounts of data in the Gbit or Tbit domain, especially when equipped with hyper-spectral cameras [3]. The ISL can be preferably operated as an optical or laser link denoted as OISL (Optical ISL) if both LEO and GEO satellites are equipped with LCTs [6,7]. The benefits of operating the ISL as OISL are: availability of high data rates (up to 1800 Mbps net rate with current LCT technology), no need for ITU spectrum regulation, robustness against interference from other systems, and no kind of harm or interference to other systems or antennas on the same platform.

A direct optical transmission on the DL from space to GS was already demonstrated as technology highlight but is commercially limited by the fact that any clouds will make the optical link unavailable, although there is considerable progress on OGS (Optical Ground Station) technology based on adaptive optics. Hence the received optical signal is split in the GEO relay into N data streams transmitted on N microwave downlinks, where N=2 or N=4 for EDRS. The Alphasat GEO launched in July 2013 contains as TDP1 (Technology Demonstration Payload number 1) also a relay element with an LCT [13] and one RF DL with N=1.

The optical signal is generated and received by optical telescopes of the LCT, implying a very narrow beam of few µrad opening, which has two consequences:

- The telescopes on both satellites have to follow the movement of the LEO satellite based on a pointing and tracking mechanism, including also a pointing-ahead mechanism since the transmit and receive beams differ considerably due to the angular speed of the LEO satellite.
- Both satellites are subject to microvibrations caused by gyro wheels and solar panels, thus mechanisms are necessary outside and inside of the LCTs to minimize the impact of those microvibrations to an acceptable minimum.

The EDRS payload is denoted “hybrid” to represent the combination of optical and microwave components. General description of numerous aspects can be found in [1,12] and an overview with focus on the data handling aspects is presented in [2].

Since LEO satellites have an operational lifetime of typically 5 years compared to typically 15 years for GEO satellites, it is essential that technologies implemented on the GEO relay do not restrict the development of new innovations for LEO satellites. Hence, for instance, an error-control encoding on the LEO shall be terminated by decoding only at GS but not at the GEO satellite. This objective is supported by performing encapsulation and re-framing operations at several instances of the satellite network. These operations and further details on the data handling schemes in LEO and GEO satellites and especially on the error-control codes and packet-oriented transmissions are described in Section III and critically reviewed in Section IV. Simulation approach and results are provided in Sections V and VI.

III. Digital Data Processing Architectures in LEO and GEO Relay Satellites

The basic data handling mechanisms of the EDRS-based satellite network are shown in Fig. 3. We consider only the return direction from LEO via GEO to GS.

- The transmission chain starts with the sources (also denoted as mass memories, MM) with data rates of about 280 Mbps. The data is organized in packets denoted as “source CADU frames” or “MM frames”. However, the MM packet structure is ignored in the LCT and subsequent stages.
- The LIAU (LCT Interface Adaptation Unit) located in the LEO performs the multiplexing of the two asynchronous source data streams, together with an encapsulation into new packets denoted as “LIAU superframes”. Furthermore, encoding, interleaving and scrambling is applied. Frame stuffing with LIAU idle frames is performed to achieve independence from the source data rates. Similarly as above, the LIAU packet structure is ignored in the LCT and subsequent stages.
- The DPU (Digital Processing Unit) located in the GEO performs another encapsulation into new packets denoted as “GEO (hyper)frames” or “DPU (hyper)frames”, together with encryption and encoding. Also again frame stuffing with GEO idle frames is applied, allowing to operate the DL with the DPU local clock and to terminate the clock of the received signal from the LEO which is subject to

a maximum Doppler offset of 27 ppm due to the relative speed of the LEO spacecraft compared to GEO spacecraft.

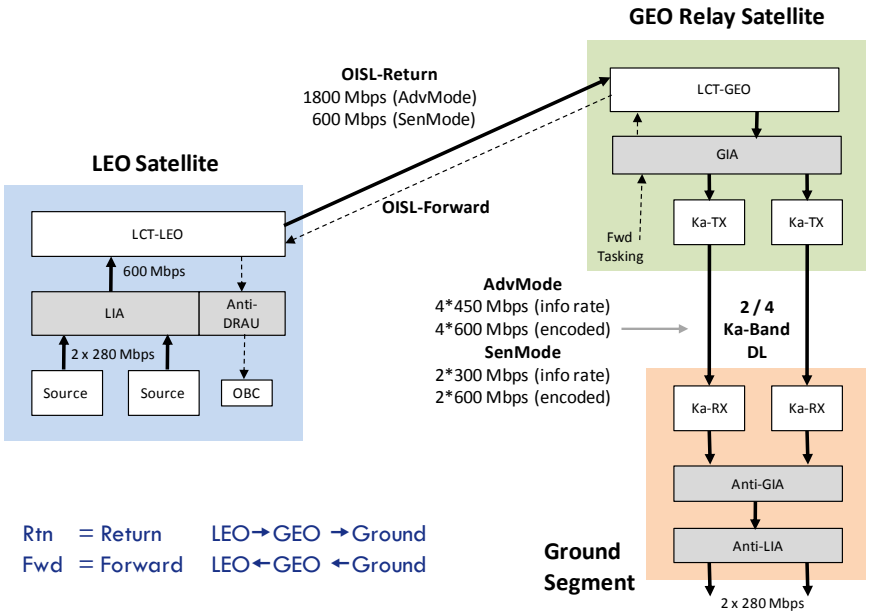

Fig. 3: Overview of data handling in LEO-GEO satellite network

		EDRS-A/C Sentinel mode	EDRS-A/C Advanced mode	Alphasat
Source (MM)	output data rate data structure frame length	~2 · 280 Mbps CADU frames 2044 bytes	tbd	~2 · 280 Mbps CADU frames 2044 bytes
LIAU	output data rate data structure frame length coding frame stuffing idle frame percentage	600 Mbps LIAU frames 2044 bytes RS(255,239) yes ~0.12%	tbd	600 Mbps LIAU frames 2044 bytes RS(255,239) yes ~0.12%
OISL	net data rate gross data rate	600 Mbps 2812.5 Mbps	1800 Mbps 2812.5 Mbps	600 Mbps 2812.5 Mbps
DPU	input data rate output data rate data structure frame length coding encryption frame stuffing idle frame percentage	600 = 2 · 300 Mbps 2 · 600 Mbps GEO frames 2044 bytes RS(255,239) * CC(2/3) AES-CBC yes ~19.41%	1800 = 4 · 450 Mbps 4 · 600 Mbps GEO frames 2044 bytes RS(255,239) * CC(5/6) no yes ~3.34%	transparent
Ka-band DL	data rate symbol rate modulation	2 · 600 Mbps 2 · 300 MBaud OQPSK	4 · 600 Mbps 4 · 300 MBaud OQPSK	1 · 600 Mbps 1 · 300 MBaud OQPSK

Tab. 1: Key data handling parameters

An overview of the basic data handling parameters is given in Tab. 1. The advanced mode with 1800 Mbps is fully supported by the current LCT technology and the EDRS-A/C payloads, but current Sentinel satellites are limited to 600 Mbps and the LIAU is not yet specified for the high-rate mode. The TDP1 of Alphasat is included for here comparison: it does not contain any DPU, so the 600 Mbps data stream received from the LCT is directly fed into the modulator.

The architecture of the LIAU is shown in Fig. 4, see also [2] for additional details. The data streams of two sources (or MMs) are multiplexed to a single data stream in the LIAU. The source data has a packet structure based on CADU frames, but this structure is ignored and the source data is considered in the LIAU as a bit stream (actually as a byte stream). This stream is divided into blocks of 1910 bytes and a header of 2 bytes is added. The header contains a 4-bit cyclic counter and is also needed to identify the ID of the source after the multiplexing operation (i.e. for demultiplexing at GS).

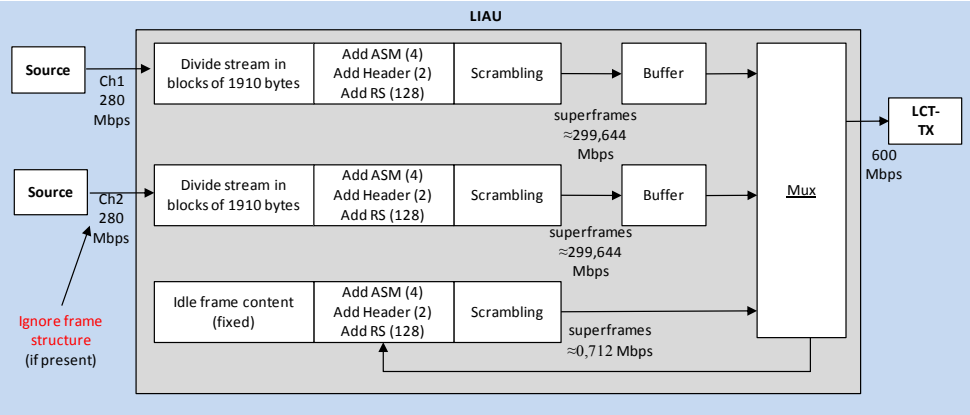

Fig. 4: Architecture of LIAU at LEO satellite

On the resulting block with a length of $1912 = 8 \cdot 239$, a (255,239) Reed-Solomon Code is applied 8 times leading to a block of $2040 = 8 \cdot 255$ bytes. Interleaving and scrambling is then performed and finally a 4-byte ASM (Attached Sync Marker) word is added resulting in a frame length of 2044 bytes. These operations are fully in line with the CCSDS standard [10] and are also similar to the CADU standard. With a data rate of 280 Mbps for each source, a data rate of $280 \cdot 2044/1910 = 299.644$ Mbps is resulting after these operations. The encoding operations are performed individually per source.

The two sequences of frames of both sources and a third sequence of idle frames are multiplexed statistically on a first-come-first-serve basis in order to achieve a fixed data rate of 600 Mbps. The small amount of idle frames with an average data rate of $600 - 2 \cdot 299.644 = 0.712$ Mbps is sufficient to terminate the clocks of the mass memories and to further proceed with the clock of the LIAU only. The idle frames are generated from a fixed pattern of 1910 bytes and the transition from 1910 to 2044 bytes is identical to the data frame processing. Of course, the header is also used to tag idle frames allowing their identification and removal on the receiver side.

Fig. 5 shows the delay distributions of MM1 and MM2 frames caused by the LIAU multiplexer. The delay is defined as time difference between the end of an incoming block of 1910 bytes and the start of the corresponding outgoing LIAU frame of 2044 bytes. The processing time is assumed to be zero, so multiplexing delays of approximately zero really occur. Note: the delay is limited approximately by the duration of 54.571 µs for the 1910-byte blocks in case of 280 Mbps for the MM data rate.

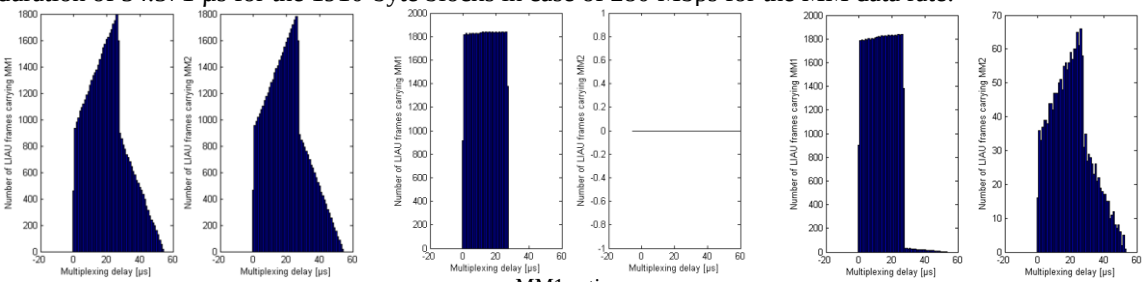

MM data rates similar but asynchronous

MM1 active
MM2 inactive

MM2 rate small compared to MM1 rate

Fig. 5: Delay distribution at LIAU multiplexer

Depending on the two modes (see Tab. 1), the OISL is operated with a net data rate of either 600 Mbps or 1800 Mbps. Independently of this, the gross data rate on the OISL between the two LCTs is always

exactly 2812.5 Mbps (with an accuracy given be LIAU local clock). From 1800 Mbps, the gross rate is achieved by a further internal LCT encoding using a (25,16) block product code and other line code operations. For 600 Mbps, this internal LCT coding is preceded by a simple (3,1)-repetition code to generate 1800 Mbps, which is mainly introduced for data rate adaptation rather than for error protection (although the repetition code relaxes the link budget as shown later).

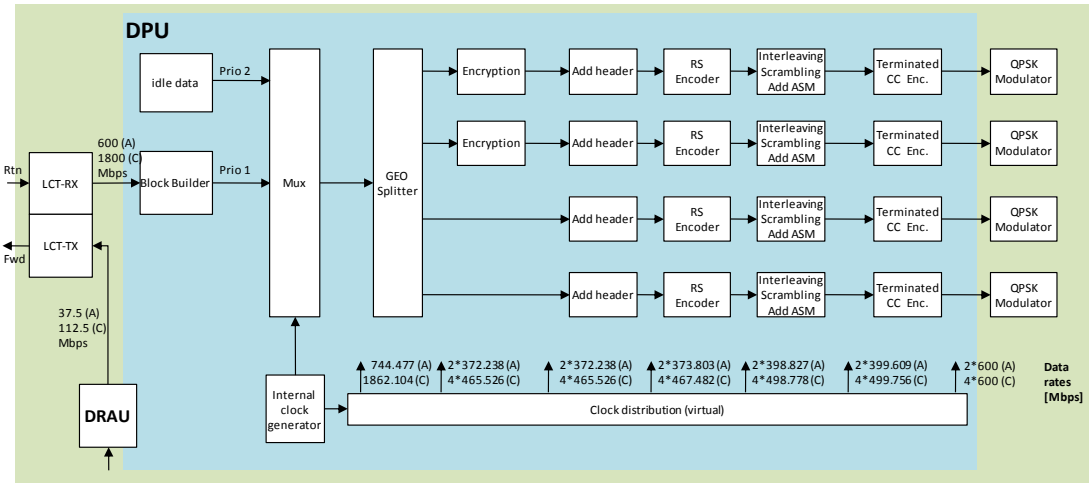

Fig. 6: Architecture of DPU at GEO satellite

The architecture of the DPU is depicted in Fig. 6 (see also [1,2] and [12] for a photo). There are some similarities and some differences to LIAU. The receiving LCT delivers a data rate of either 600 or 1800 Mbps to the DPU. The data rate is subject to a change with a maximum of 27 ppm due to the Doppler shift caused by the movement of the LEO satellite relative to the GEO satellite.

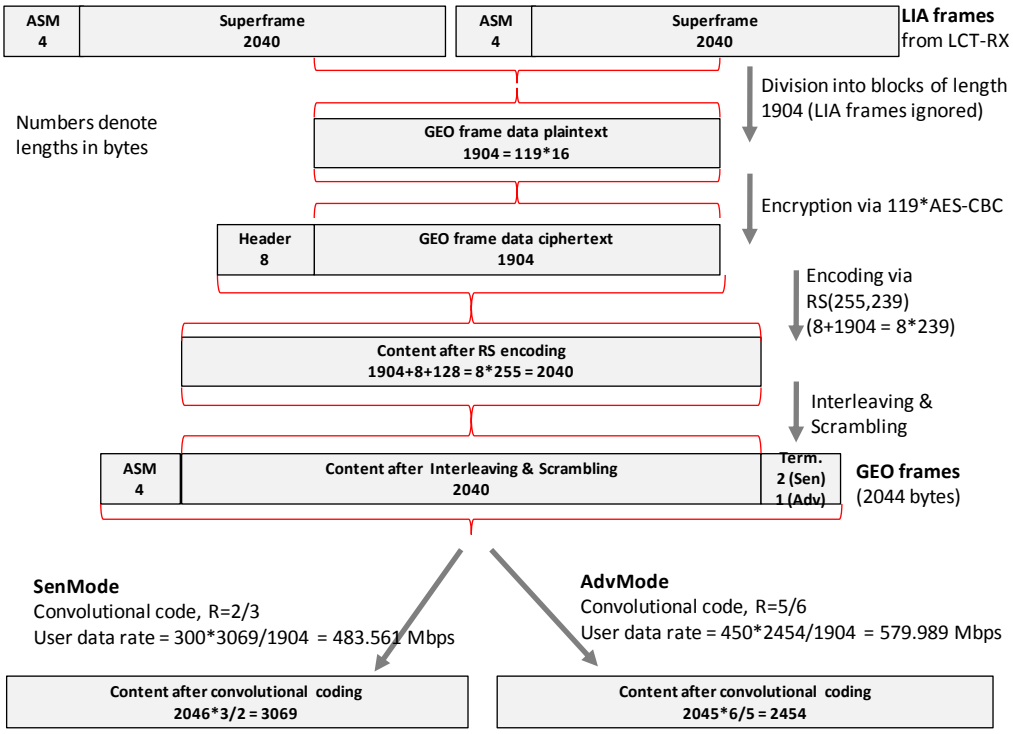

Fig. 7: Framing operations in DPU

As shown in Figs. 6 and 7, the incoming data stream from LCT is divided into blocks, ignoring the present LIAU frame structure. Encryption is applied with a block cipher operated in CBC (Cipher Block Chaining Mode). In the next steps, a header is added, ciphertext and header are RS encoded, followed by interleaving and scrambling and addition of ASM. Finally, convolutional coding is applied with code rates of 2/3 and 5/6 for Sentinel and Advanced modes, respectively. The resulting data rates are 483 and 580 Mbps per DL channel, and the gap to 600 Mbps as the gross bit rate per DL channel is filled with GEO idle frames.

In case of Sentinel mode, the DL is operated with 19.41% stuffing overhead by idle frames (see also Tab. 1). Since this seems to be an amazing wastage or inefficiency on the first view, an analysis was performed indicating that a rate-9/16 convolutional code is possible as alternative providing an extra gain of about 0.4 dB compared to rate-2/3. However, since this is not a standardized coding scheme with heritage, the rate-9/16 alternative was withdrawn.

Note that the frame structure is preserved throughout all stages of DPU processing. On the receiver side, the data streams from the N DL channels have to be multiplexed (inverse operation to split operation in the DPU), this is supported by insertion of cyclic frame counter in the frame header. Moreover, for additional robustness, by frame offsets in the order of T_{frame}/N between the frames on the N DL channels where T_{frame} denotes the length of a GEO frame. The N DL channels with gross data rate of 600 Mbps each are modulated for both modes with OQPSK (offset QPSK) and a symbol rate of 300 MSps, resulting in a bandwidth of 450 MHz per channel.

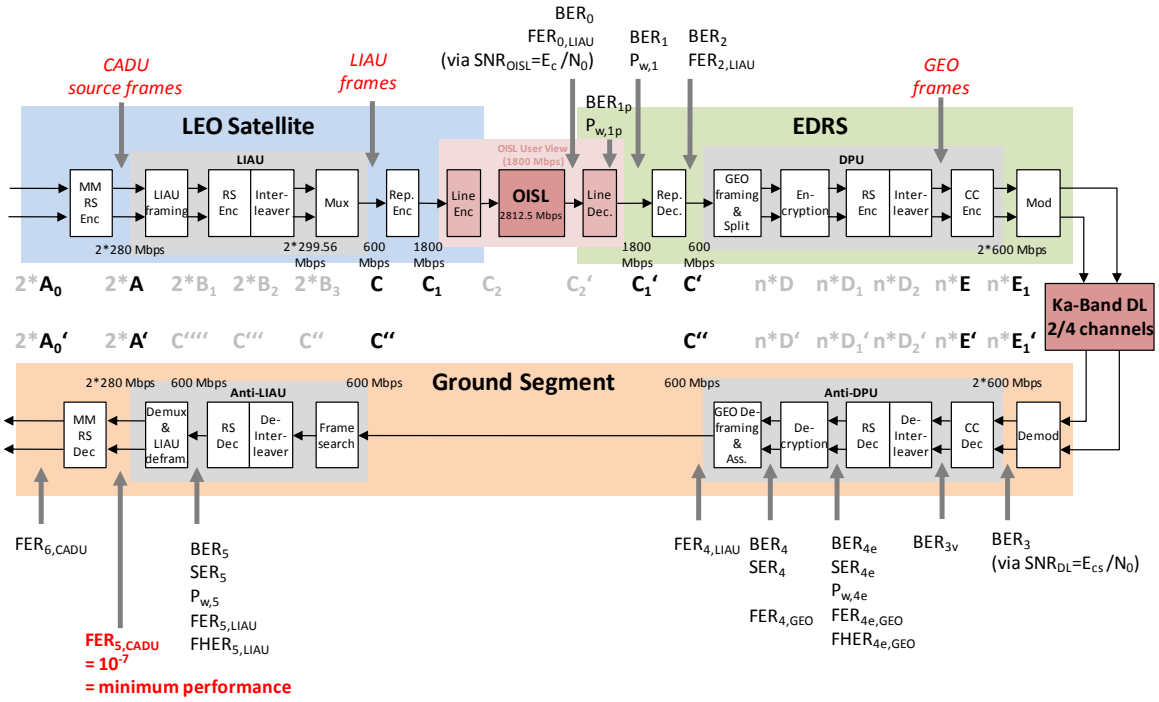

Fig. 8: System Overview in terms of error-control coding

All coding schemes are summarized in Fig. 8. Several reference points or pairs of reference points are defined. BER, SER, WER=P_w, FER, FHER denote bit-, symbol-, word- and frame- and frame header error rates. Note that the reverse operations of LIAU and DPU are denoted by the prefix "Anti-". This figure is the centerpiece representation of all digital processing in the satellite network comprising LEO, GEO and GS.

For the commercial application of EDRS, the target requirement is $\text{FER}_{5,\text{CADU}}=10^{-7}$.

IV. Critical Review of Selected Data Handling Schemes

We consider in this section various features of the selected coding schemes and other mechanisms. However, for the final assessment in the concluding Section VII, some further aspects have to be taken into account.

A) Simple Considerations on the "Concatenation" of RS Codes: The detailed interaction of the coding schemes contained in the overall chain from user application to user application is quite challenging, however, a rough overview is easier and intelligible. The results are shown in Fig. 9 (some statements made here will be confirmed later in Section VI on simulation results).

The GEO relay scenario considered throughout this paper is shown in the middle of Fig. 9. As already mentioned in Section III, the frame structures after MM and LIAU are very similar and the coding scheme is even identical. Hence, the LIAU performs a "RS on RS" operation together with the encapsulation, re-framing and stuffing operations.

Note that this "RS on RS" is not a concatenation of block codes in the usual sense. The frames after MM and LIAU both have a length of 2044 byte, but the information word at the input of the coding sections is smaller, e.g. 1910 bytes at LIAU input. Hence, one MM frame is encapsulated by two LIAU frames at least and three LIAU frames at most. In other words, the frame boundaries of LIAU frames and MM frames are sliding but not aligned. The lengths of the MM and LIAU frames are identical in bytes, but LIAU frames are shorter in time since the data rate is higher. A LIAU frame is even shorter in time than half of the MM frame since the LIAU is multiplexing two MMs.

Similar considerations apply for the DPU encapsulation, hence the DPU is operated as "RS on RS on RS". Again, GEO frames after DPU RS encoding have an identical length in bytes as LIAU frames, but GEO frames are shorter in time.

Let us consider the decoder operations in the middle of Fig. 9 by skipping the convolutional code (CC). The DPU RS code is used for the protection of the DL, errors on the OISL are invisible for DPU RS. The LIAU RS could be used in theory for the protection of both DL and OISL, but effectively the DL is not (or only slightly) protected by the LIAU RS due to the following reason: If errors caused by the DL are remaining after the DPU decoder, then the error structures are such that the LIAU RS decoder correction capability will be typically exceeded (this applies even more if a block cipher like AES is applied in between). The situation could be changed if a deep interleaving over several frames is applied at the DPU input. With a similar argument, the MM RS code is more or less inefficient, both with regards to OISL or DL errors, however, for error detection on the user layer the MM RS could be beneficial.

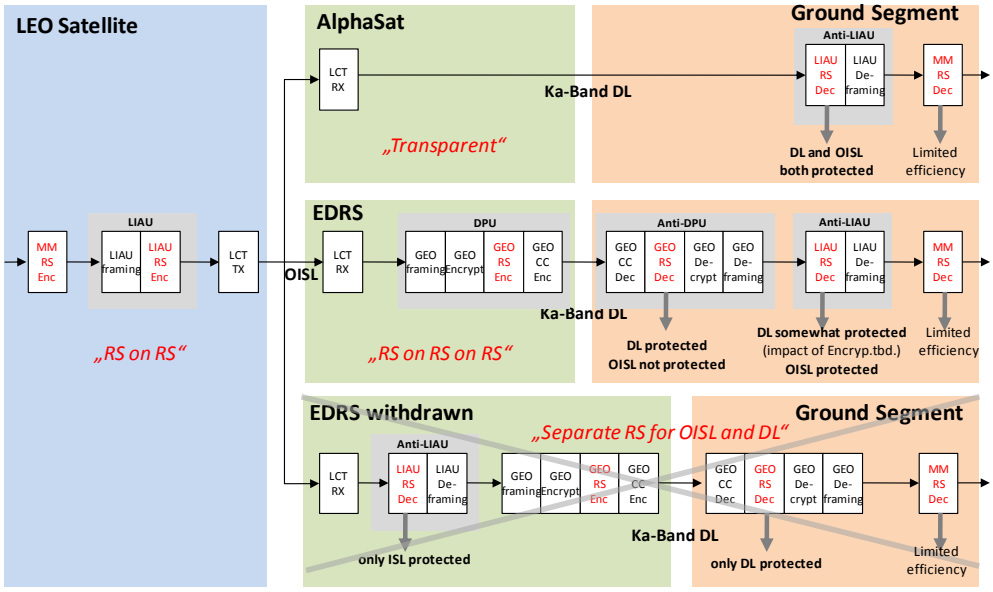

Fig. 9: Specific capabilities of error-correction codes

An alternative to this "RS on RS on RS" approach in the DPU is shown in the lower part of Fig. 9, where the LIAU RS code is terminated in the GEO satellite. Here, the DPU performs decoding for the first link and encoding for the second link. This approach was withdrawn, because this implies a footprint of the specific LEO technology on the GEO satellite; also a decoder operation in space is required.

The upper part of Fig. 9 shows the situation with Alphasat TDP1 as GEO data relay. Alphasat TDP1 is transparent without any kind of digital data processing. In this case, the LIAU RS code is used to correct both errors caused by OISL or DL, but the MM RS is rather inefficient as for the other cases.

B) Interleaving: Since the error structure of the OISL is characterized by independent bit errors with constant error rate per GEO frame, the selected well-known RS code with interleaving over 8 RS words is not the optimum coding scheme, but the potential improvements due to other coding schemes for hard-decision channels are not overwhelming.

The conventional standard interleaving scheme defined in [10] is not the optimum since (i) the frame header is more important than the remaining data part of the GEO frame and (ii) due to the interaction with encryption as discussed in [2].

C) Frame type classification: The GEO frame type classification in the receiver (de-stuffing) could be based on the frame type indicator contained in the header. The robustness can be enhanced by a correlation method described in [2].

D) Is the FER a reasonable measure to assess system performance? Obviously, the performance of the system should be based on frame error rates. However, for a sensible assessment of the system properties the statistical distribution of wrong frames should be considered as well, e.g.:

- Does it matter if there is a difference between "every session has few wrong frames" and "most sessions are error-free but few sessions have many wrong frames"?
- Is it reasonable to count the loss of a frame (missing bits) in the same way as the distortion of a frame (wrong bits but same number of bits)? Or should a loss be considered as more dramatically than a distortion?

However, the appropriate definition of performance should depend on the end-user requirements.

V. Simulation Approach

Fig. 10 describes the approach for the performance assessment via simulation. The grey-colored boxes represent the data processing in LEO, GEO and GS, the red boxes represent the two transmission channels. The microwave DL is quite easy to model, in rough approximation it can be considered as AWGN (Additive White Gaussian Noise) channel, where the noise power is time-invariant under clear sky conditions and time-variant in case of rain fading. Linear distortions due to channel filters in waveguide technology and nonlinear distortions due to power amplifiers with travelling wave tubes operated in saturation need to be represented approximately by adequate SNR degradations.

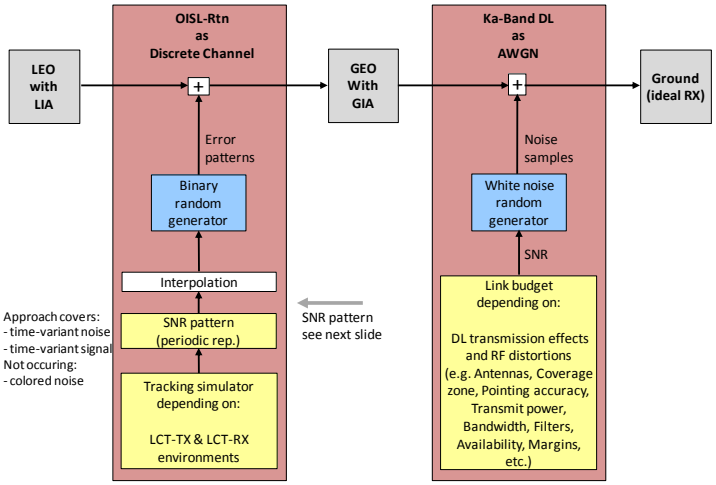

Fig. 10: Performance Assessment via simulation approach

A model for the error structure of the OISL is more challenging than for the DL. The noise in the optical receiver can be represented as white (statistically independent noise samples) with time-invariant noise power. The received signal power is time-variant due to the microvibrations of both satellites. A model for

the tracking of microvibrations was developed based on vibration spectra at the mechanical interface of the LCT for both LEO and GEO satellite busses. A SNR pattern is generated from the simulated signal pattern and the noise pattern as shown in Fig. 11.

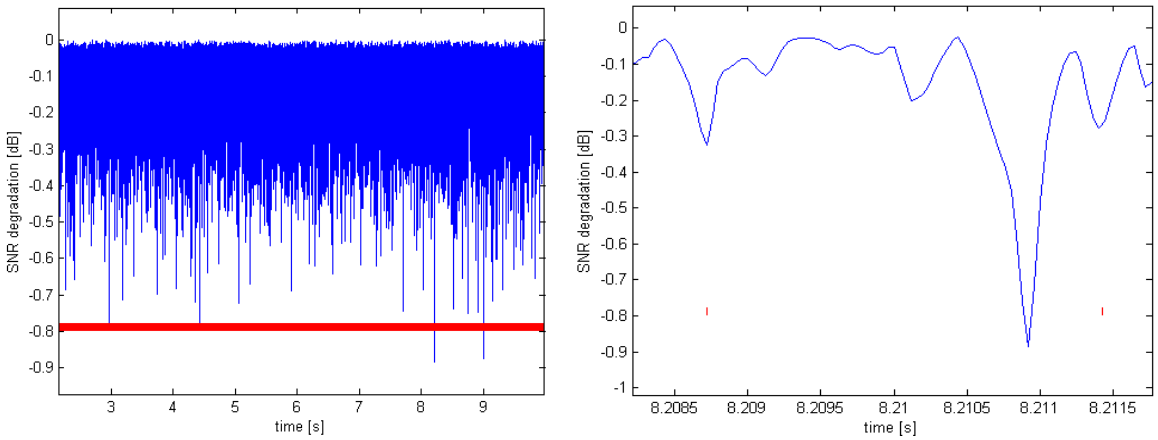

Fig. 11: Example of OISL SNR pattern
(over 7850 ms @left, time interval of 3.5 ms around the deepest fade enlarged @right)

Fig. 11 shows the SNR pattern over several seconds in the left part. Obviously, 13.5 dB is the best case and the worst case is about 1 dB less. The time scale is enlarged in the right part to study the time around the deepest fade in more detail. The short vertical red lines indicate the duration of 100 LIAU frames. Compared to a single LIAU frame, the SNR variations are approximately time-invariant within a frame. Hence the OISL is a simple binary channel with independent bit errors and time-invariant BER during the duration of a frame.

The simulation results reported in Section VI are displayed over a fixed SNR_{OISL}, i.e. the patterns from Fig. 11 with the small SNR_{OISL} variations are not used at all for the simulation. If future OISL setups with other microvibration environments are characterized by large but slow time-variant SNR, then the performance of such time-variant OISLs can be calculated from the present performance results for time-invariant OISLs as summarized in Fig. 12.

Word-error rate: $P_w(\gamma) = P(\text{word error} \mid SNR_{OISL} = \gamma)$

Let f_γ be the PDR of $\gamma = SNR_{OISL}$

The overall WER is the expected value of the conditional probability:

$$P_w = E(P_w(\gamma)) = \int_{-\infty}^{+\infty} P_w(\gamma) \cdot f_\gamma(\gamma)\, d\gamma \approx \sum_i P_w(\gamma_i) \cdot f_\gamma(\gamma_i)$$

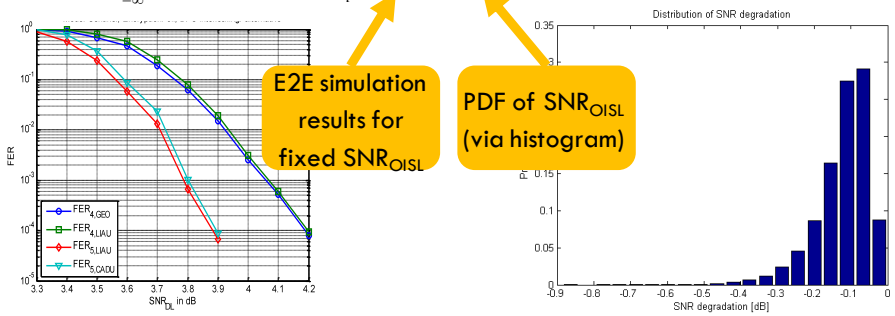

Fig. 12: From time-invariant OISL results to time-variant performance

VI. Simulation Results

We have introduced in Fig. 8 various types of error rates like BER, SER, WER, FER, FHER between various reference points like C-C', E-E', C-C''', C-C'''' and A-A'. All these error rates (and additional LCT-internal error rates not shown in Fig. 8) have been simulated

- for Sentinel and Advanced mode,
- with and without encryption,
- with standard and alternative interleaving schemes,
- for different alignments between CADU, LIAU, GEO frames (56 different alignments are possible),
- for different asynchronous and synchronous MM data rates and
- for various Doppler shifts.

The simulation results were analyzed and the relations between the error rates show a very good match with the analytically derived relations. Methods for runtime acceleration as described in [2] have been partly applied, however even with simulation stops at error rates in the order of 10^{-5} or 10^{-7} final conclusions can be drawn since error-floor effects only occur due to implementation losses but not due to error-control decoding algorithms (no iterative decoding).

A selection of some simulation results is reported below and displayed over the signal-to-noise ratios SNR_{OISL} and SNR_{DL} of the two links.

Fig. 13 displays BER and FER values at various reference points over SNR_{OISL} under the assumption of an error-free DL and for Sentinel mode (i.e. with enabled LCT repetition code). The FER_5 of LIAU and CADU frames after the Anti-LIAU are almost identical, the remaining small difference is not caused by coding but only by the re-framing operation and is limited to

$$FER_{5,CADU} \leq 2 \cdot FER_{5,LIAU}$$

The BER_5 at the same point is smaller by several magnitudes since a frame consists of 2044 bytes. The BER_0 of the uncoded OISL is equivalent to

$$BER_0 = Q(\sqrt{2 \cdot SNR_0})$$

FER_2 is defined as LCT-protected LIAU FER of the OISL and thus the extreme difference to FER_5 is due to the protection provided by the LIAU RS code.

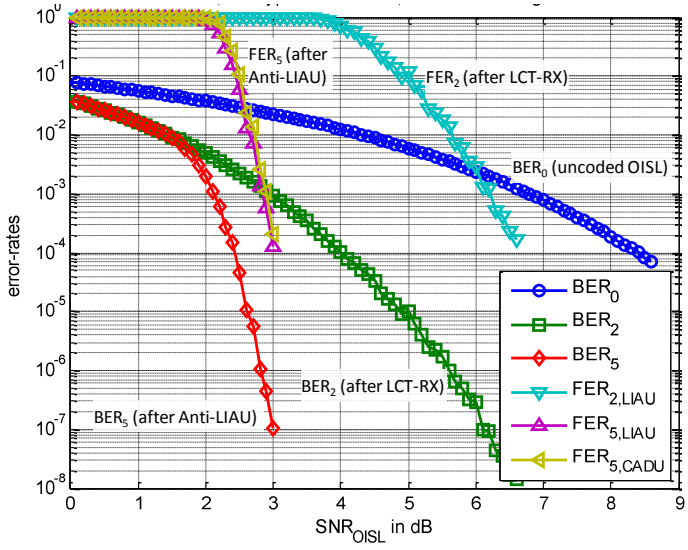

Fig. 13: BER and FER over SNR_{OISL} (DL perfect, Sentinel mode)

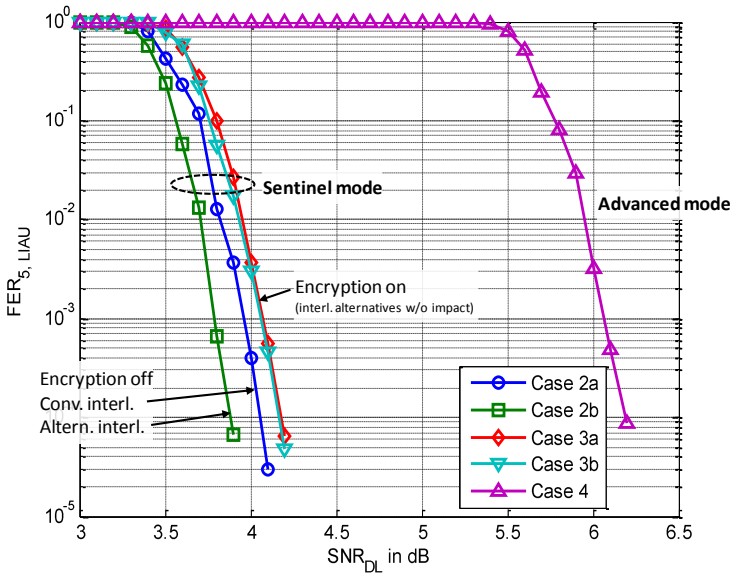

Fig. 14: $FER_{5,LIAU}$ over SNR_{DL} (OISL perfect, Sentinel & Advanced mode)

Fig. 14 displays $FER_{5,LIAU}$ over SNR_{DL} for Sentinel and Advanced modes under the assumption of an error-free OISL. The Advanced mode requires several dB more SNR on the DL compared to the Sentinel mode since the convolutional code rate is larger (the disabled repetition code of the LCT has no impact in case of perfect OISL).

The activation of the encryption causes an additional loss due to AEC-CBC error propagation. This loss would be equivalent to a factor of 65 in case of statistically independent errors, however, for the scenario under consideration the error structure is more complex after the RS decoder in the Anti-DPU. A detailed analysis and the simulation indicate that a change of the RS interleaving scheme as discussed in [2] would reduce the encryption loss. Nevertheless, the standard interleaving scheme as recommended by CCSDS [10] is applied in the DPU.

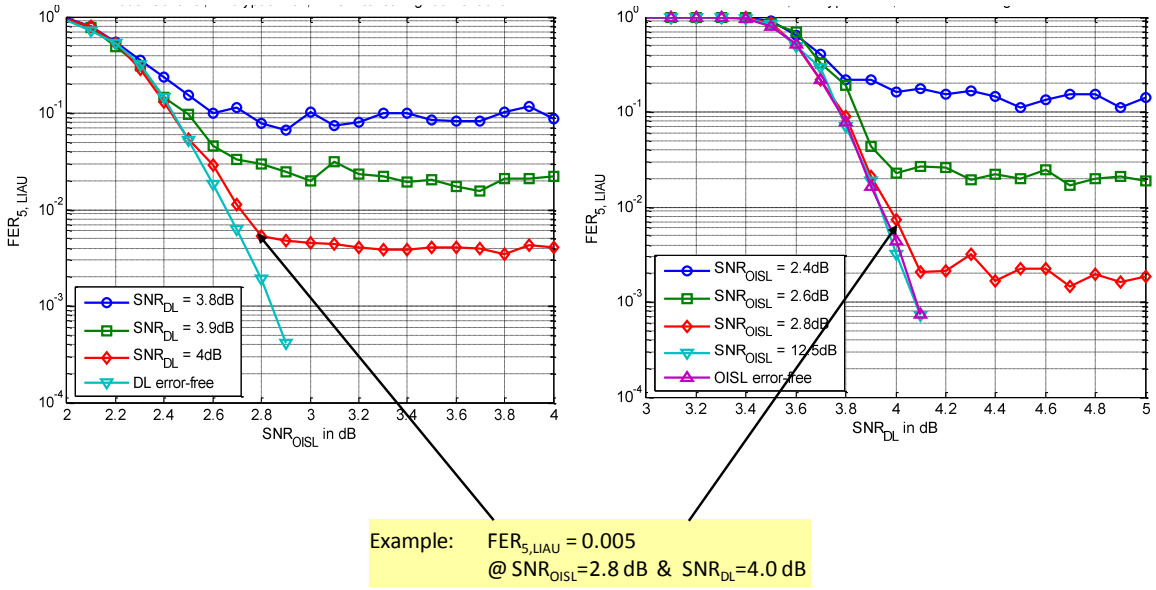

Fig. 15: FER over SNR_{OISL} and SNR_{DL} (Sentinel mode)

Fig. 15 displays $FER_{5,LIAU}$ over SNR_{OISL} and SNR_{DL} in case of Sentinel mode. Of course, each of the links causes an error floor effect to the other link. The zig-zag look in the right plot is a good indication for insufficient simulation runtime, however this has no impact on the basic conclusions.

A more detailed analysis shows that link-individual error rates under the assumption that the other link is perfect cannot be added to generate the total error rate, i.e. the relation

$$FER_{5,LIAU,combined} = FER_{5,LIAU,perfectDL} + FER_{5,LIAU,perfectOISL}$$

is not confirmed by the simulations. The effects behind this are not yet completely understood, even considering that the LIAU RS code also helps to protect the DL and that error rates are not additive for the concatenation of fully independent memoryless channels.

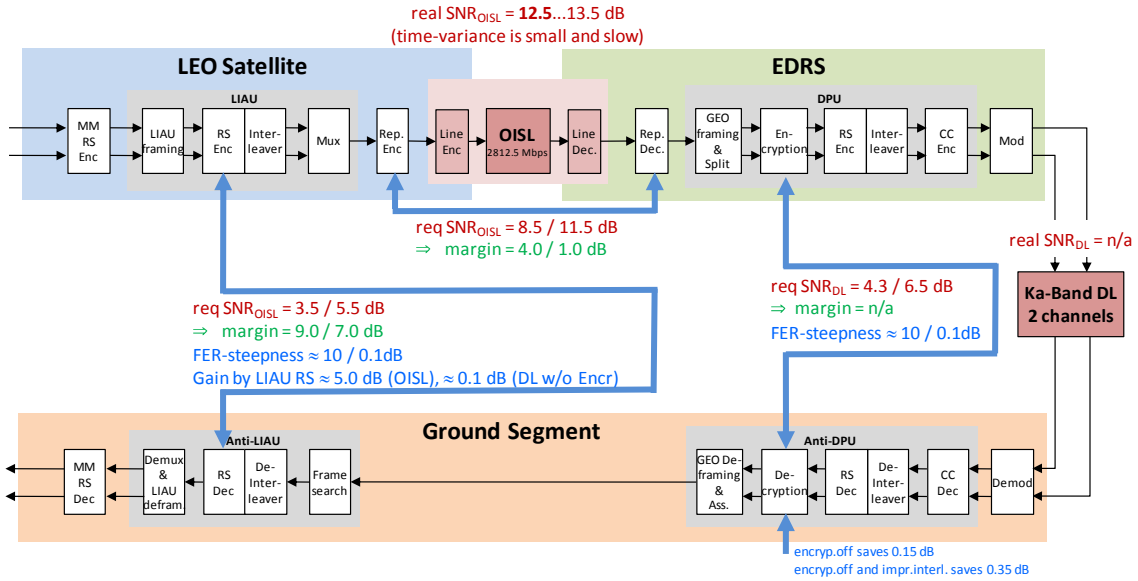

Fig. 16: Link budget summary (numbers refer to Sentinel/Advanced mode)

The main results of the EDRS performance assessment are summarized in Fig. 16. For a frame error rate of about 10^{-7} after the Anti-LIAU as service level objective, the OISL requires an SNR_{OISL} of 8.5 / 11.5 dB for Sentinel/Advanced mode and the DL requires an SNR_{DL} of 4.3/6.5 dB. Non-surprisingly, the FER graphs are very steep for both links. It is also interesting to note that the LIAU RS code contributes to a very small amount of 0.1 dB to the protection of the DL transmission.

VII. Conclusions

The performance of the EDRS satellite network was successfully analyzed with regards to the error rates associated to the digital data transmission schemes. The most important results are:

- The link margin for the OISL is large for the Sentinel mode, but smaller for the Advanced mode. This has to be taken into account for the design of the 1800 Mbps LIAU. The microvibration issue causes no severe performance degradation.
- The link margin for the DL cannot be commented here since this depends on various parameters like coverage area, availability and ground antenna gain, all being under the responsibility of Astrium Services (ASV) but not in the scope of Tesat-Spacecom.

The interaction between all coding schemes, framing and reframing operations and the relations between various packet error rates is so complex that analytical consideration have to be supplemented by Monte-Carlo simulations. In case of overlapping between theory and simulation, there is a perfect match between both. New insights were derived regarding the LCT codes (not fully described here), the concatenation of RS codes and the impact of block cipher encryption on the error structures.

It is emphasized that the selection of the data handling schemes was done under various constraints, including the technology independence of the GEO relay from future LEO evolutions, the availability and heritage of existing technology in the areas of mass memories, LCT and modulators. Thus, the selection of the modulation and coding scheme should not be misinterpreted as the result of an overall coding-centered optimization!

The frame based transmission with stuffing involves specific error scenarios being new for the satellite communications community. It is essential that de-stuffing in the GS (i.e. the differentiation between data frames and idle frames) is done such that catastrophic error propagation is avoided. The author of this paper had the chance to contribute to the development of the digital algorithms in the GS.

As a lesson from the EDRS development process, it is important to start the design of the ground segment not later than the one for the space segment. Insights from the receiver development could have impact on the transmitter specification. For instance, the headers of LIAU and GEO frames were specified 1...2 years prior to the GS design, and some parameters in the header fields have now turned out as useless. However, the impact on the signaling overhead is negligible.

We conclude with a look on the evolution of next generation hybrid payloads, mainly from the coding point of view (some additional areas for further evolution are listed in [1]):

- The first step towards more efficient relay satellites is the introduction of advanced coding and modulation schemes like 16/32/64-APSK [1,11] and the replacement of the traditional RS*CC concatenated code by more efficient schemes like SCCC (Serial Concatenated CC) or LDPC (Low Density Parity Check Code). Adaptive operation is possible (e.g. depending on the DL conditions), either by storage of data within the GEO relay or by flow-control (backpressure) of the source in the LEO spacecraft.
- Alternatives for coding also could include PLC (Packet Level Coding) [9] or delay-tolerant ARQ protocols to master interruptions due to potential link losses or re-acquisitions of the optical link [9] (or could also be applied to the DL).
- GEO relays are expected to be equipped with several LCTs in future to enable GEO-GEO optical connectivity (over 85000 km, requiring an LCT polarization shift) in order to provide global coverage, preferably together with a transition from the current DPU functionality towards increased routing capabilities. This implies also the transmission of high data rates in both directions of the OISL.
- The LIAU coding should be improved or alternatively the LIAU and the mass memories will be integrated into one unit, also requiring other reference points for the specification of the service level key parameters. The encryption could be shifted from GEO to LEO satellites for a real end-to-end privacy approach.

References

[1] W.Lütke: Hybrid Optical/RF Payloads for Current and Future Datalink Applications, ICSSC 2013 (to be publushed), Florence, Italy, Oct. 2013.

[2] B. Friedrichs, P.Wertz: Error-Control Coding and Packet Processing for Broadband Relay Satellite Networks with Optical and Microwave Links, 6th Advanced Satellite Multimedia Systems Conference (ASMS 2012), Baiona, Spain, Sept. 2013.

[3] U.Lonsdorfer, F.G.Rombeck: High Speed CCSDS Data Formatter, Proceedings of DASIA 2003 (ESA SP-532). 2-6 June 2003, Prague, Czech Republic, p.35.1

[4] J.Aschbacher, M.P.Milago-Perez: The European Earth (GMES) Programme – Status and Perspectives. GMES Space Office, February 2012.

[5] www.gmes.info

[6] F.Heine, H.Kämpfner, R.Lange, R.Czichy, R.Meyer, M.Lutzer: Optical Inter-Satellite Communication Operational. The 2010 Military Communications Conference, pp. 2284-2288.

[7] F.Heine, H.Kämpfner, R.Lange, R.Czichy, R.Meyer, M.Lutzer: Laser Communication Applied for EDRS, the European Data Relay System. CEAS Space Journal, Vol.2, Numbers 1-4, pp.85-90.

[8] A.Hegyi: EDRS – Die Datenautobahn im Weltraum. 3.Nationale Konferenz Satellitenkommunikation, März 2012, Bonn, Deutschland.

[9] G.Garrammone, B.Matuz, G.Liva: An Overview of Efficient Coding Techniques for Packet Loss Recovery om CCSDS Telemetry Links. 5th ESA Workshop on Tracking, Telemetry and Command Systems for Space Applications, TTC 2010, September 2010, Noordwijk, Netherlands.

[10] TM Synchronization and Channel Coding, Recommendation for Space Data System Standards, CCSDS 131.0-B-2, Blue Book, Washington, D.C.: CCSDS, August 2011

[11] P.Wertz, S.Mauch, B.Friedrichs: High Data Rate Transmission for Earth Observation Missions using Next Generation Downlink Subsystems, ICSSC 2013 (to be publushed), Florence, Italy, Oct. 2013.

[12] N.LeGallou, W.Lütke, A.Camuso, B.Wittwer, M.Leadstone, H.Schuff, J.-P.Cousty, B.Folio, A.Murrell: The EDRS-A and EDRS-C Data Relay Payloads, ICSSC 2013 (to be publushed), Florence, Italy, Oct. 2013.

[13] G.Mühlnikel, H.Kämpfner, F.Heine, H.Zech, D.Troendle Tesat, R.Meyer, S.Philipp-May: The Alphasat GEO Laser Communication Terminal Flight Acceptance Tests, Proc. International Conference on Space Optical Systems and Applications (ICSOS) 2012, 13-1, Ajaccio, Corsica, France, October 2012.